

Modeling and Control of a Photovoltaic Energy System Using the State-Space Averaging Technique

¹Mohd Saifuzam Jamri and ²Tan Chee Wei

¹Department of Power Electronics and Drives, Faculty of Electrical Engineering,
University Tekikal Malaysia Melaka, Malaysia

²Department of Energy Conversion, Faculty of Electrical Engineering,
University Technology Malaysia, Malaysia

Abstract: Problem statement: This study presented the modeling and control of a stand-alone Photovoltaic (PV) system using the state-space averaging technique. **Approach:** The PV module was modeled based on the parameters obtained from a commercial PV data sheet while state-space method is used to model the power converter. A DC-DC boost converter was chosen to step up the input DC voltage of the PV module while the DC-AC single-phase full-bridge square-wave inverter was chosen to convert the input DC comes from boost converter into AC element. The integrated state-space model was simulated under a constant and a variable change of solar irradiance and temperature. In addition to that, maximum power point tracking method was also included in the model to ensure that optimum use of PV module is made. A circuitry simulation was performed under the similar test conditions in order to validate the state-space model. **Results:** Results showed that the state-space averaging model yields the similar performance as produced by the circuitry simulation in terms of the voltage, current and power generated. **Conclusion/Recommendations:** The state-space averaging technique is simple to be implemented in modeling and control of either simple or complex system, which yields the similar performance as the results from circuitry method.

Key words: Photovoltaic, state-space averaging, boost converter, single-phase square-wave inverter

INTRODUCTION

Solar energy as one of many favored renewable energy resources has become an important part of power generation in the new millennium. The first conventional photovoltaic cells were produced in the late 1950s and throughout the 1960s were principally used to provide electrical power for earth-orbiting satellites. Photovoltaic (PV) systems produced electricity when the photons of the sunlight strike on the PV array. Solar energy is environmental friendly and which generates electricity without hazardous emissions. Furthermore, the sunlight is free and it is available for long hours in a day throughout the year in Malaysia.

The PV application can be categorized as grid connected system, stand-alone system and hybrid system. The stand-alone PV system is defined as an autonomous system that supplies the electricity without being connected to the utility grid. The installation of the system may include PV array, DC-DC converter, energy storage device, DC-AC inverter and an electrical

load. The energy storage device is used to maintain the desired output during the low irradiance or during the night time. Many works have been done in the PV system simulation and modeling. The issue of PV modeling has been discussed in (Theocharis *et al.*, 2005; Ito *et al.*, 2003; Ropp and Gonzalez, 2009; Salhi, 2009; Bae *et al.*, 2005; Armstrong and Hurley, 2004).

This study focuses on modeling and control of a stand-alone photovoltaic system using the state-space averaging technique without the connection with energy storage device. The state-space representation approach is a mathematical model that capable of describing the system averaged behavior as the input, output and state variables regarding to any linear or nonlinear system. The electrical system can be modeled using the state-space averaging method, where it can be classified as the linear system since we can find the states of the system for all time $t > t_0$ for a given set of input sources (Chen, 1999).

The stand-alone photovoltaic system modeled using the state-space averaging method has the advantage of simpler simulation and faster convergence

Corresponding Author: Mohd Saifuzam Jamri, Department of Power Electronics and Drives, Faculty of Electrical Engineering, University Tekikal Malaysia Melaka, Malaysia

rate as compared to the circuitry simulation. This is because the state-space averaging method does not include an active device or component in such that is used in the circuitry method.

This study begins with the description of modeling process and simulation work. Then, the simulation results will be shown and discussion of the results will be made. In addition, a similar proposed PV system which is in the form of circuitry is simulated using MATLAB/Simulink will be used to compare with the results obtained from the proposed state-space PV system. Finally, conclusion will be drawn.

Modeling and simulation:

Modeling of photovoltaic generation: Photovoltaic cell is a non-linear device and can be represented as a current source in parallel with diode as shown in the circuit in Fig. 1 (Villalva *et al.*, 2009).

The practical PV cell model includes the connection of series and parallel internal resistance, namely R_s and R_p , which is expressed as the following equation:

$$I = I_{PV,cell} - I_0 \left[\exp\left(\frac{V + R_s I}{V_t a}\right) - 1 \right] \tag{1}$$

Where:

- I = The photovoltaic output current
- V = The photovoltaic output voltage
- $V_t = N_s k T / q$ = The thermal voltage of array with N_s cells connected in series
- q = The electron charge ($1.60217646 \times 10^{-19} \text{ C}$)
- k = The Boltzmann constant ($1.3806503 \times 10^{-23} \text{ J K}^{-1}$)
- T = The temperature of the p-n junction in the unit of Kelvin
- K and a = The diode ideality constant (Villalva *et al.*, 2009)

The $I_{PV,cell}$ is the light generated current produced by a photovoltaic cell which has a linear relationship with the solar irradiance and temperature, as shown in the following equation:

$$I_{PV,cell} = (I_{PV,n} + K_i \Delta T) \frac{G}{G_n} \tag{2}$$

where, $I_{PV,n}$ is the light generated current at the nominal condition which are 25°C and 1000 W m^{-2} , $\Delta T = T - T_n$ where T and T_n is the actual and nominal temperature in unit Kelvin, K respectively. While $G \text{ (W m}^{-2}\text{)}$ is the solar irradiation by the PV surface and G_n is the nominal solar irradiation (Villalva *et al.*, 2009).

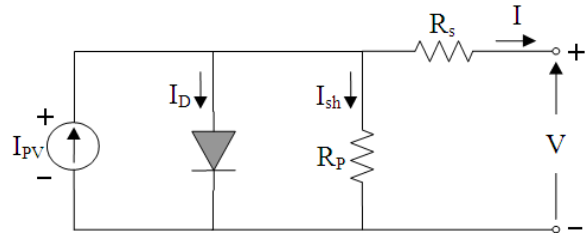


Fig. 1: The electrical equivalent circuit of a PV cell

Table 1: The electrical characteristic of BP340 PV module

Parameter	Variable	Value
Maximum power	P_{mpp}	40 W
Voltage at P_{max}	V_{mpp}	17.3 V
Current at P_{max}	I_{mpp}	2.31 A
Short-circuit current	I_{sc}	2.54 A
Open-circuit voltage	V_{oc}	21.8 V
Temperature coefficient of open-circuit voltage	K_v	$-(80 \pm 10) \text{ mV}/^\circ\text{C}$
Temperature coefficient of short-circuit current	K_i	$(0.065 \pm 0.015)\% / ^\circ\text{C}$

The diode saturation current, I_0 and its dependence on the temperature may be expressed by:

$$I_0 = \frac{I_{sc,n} + K_i \Delta T}{\exp\left(\frac{V_{oc,n} + K_v \Delta T}{a V_t}\right) - 1} \tag{3}$$

where K_v and K_i is the open-circuit voltage/temperature coefficient and the short-circuit current/temperature coefficient. While I_{sc} and $V_{oc,n}$ are the short-circuit current and open-circuit voltage under the nominal condition respectively. The BP340 solar module is chosen for the PV module modeling. The electrical characteristics given by datasheet are shown in Table 1. This module consisting of 36 cells connected in 2 parallel strings. The model of PV module was implemented in MATLAB/Simulink using Eq. 1-3. The model yields the PV current I , using the electrical parameter of the module (I_{sc} , V_{oc}) and the variables Voltage, Irradiation (G) and Temperature (T) as the inputs to the model.

The simulated I-V and P-V characteristic curves are shown in the Fig. 2 and 3 respectively, where the model is simulated for a series of solar irradiances and different temperatures. The results show that the PV module is capable of reproducing the electrical characteristics as mentioned in Table 1.

State-space averaging model for boost converter:

The typical DC-DC boost converter is shown in Fig. 4, where the output voltage is defined by the following equation:

$$V_o = \frac{1}{1-D} V_{in} \tag{4}$$

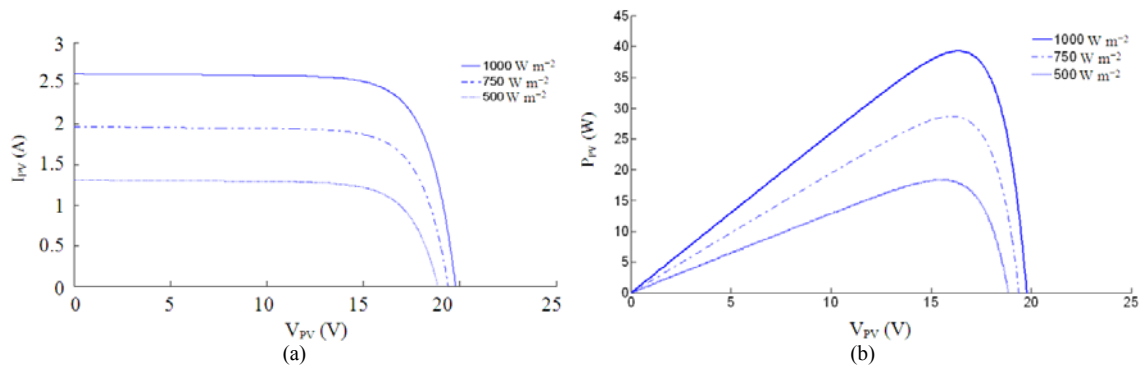


Fig. 2: PV module characteristic curves plotted under different irradiances, (a) I-V curve; (b) P-V curve

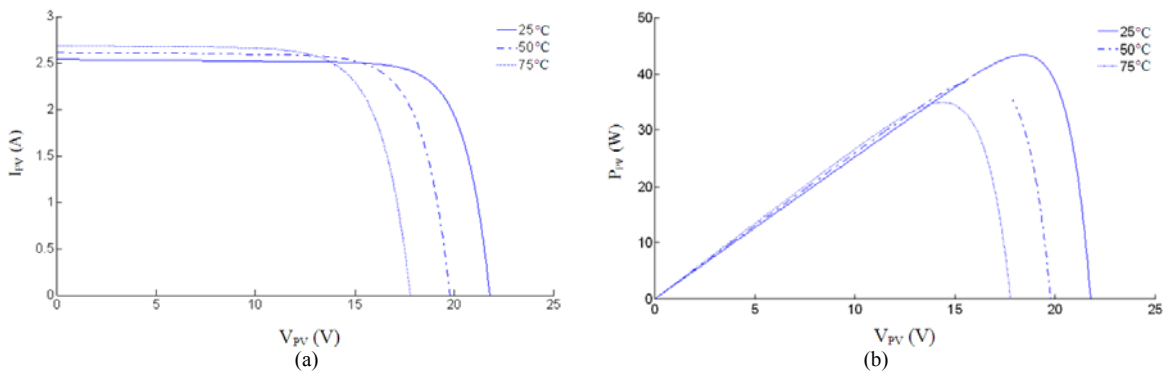


Fig. 3: PV module characteristic curves plotted for different temperatures, (a) I-V curve; (b) P-V curve

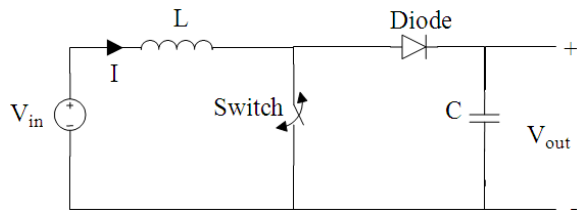


Fig. 4: The schematic diagram of a Boost converter

The state-space technique can be used to describe the behavior of a DC-DC boost converter which yields the average output value with respect to the signal behavior of switching converters, in terms of a set of linear time invariant state equations driven by a continuous duty ratio modulation function. The operation of the state-space model is described by the following basic state equations (Rashid, 2004; Moussa and Morris, 1990):

$$X(t) = Ax(t) + Bu(t) \tag{5}$$

$$Y(t) = Cx(t) + Du(t) \tag{6}$$

Where:

$x(t)$ = The state variable

$u(t)$ = The input vector

Equation 6 is referred as the output equation. Parameter A is the state matrix, parameter B is the input matrix, while C the output matrix and D is the transition matrix.

In an electrical system, the method to identify the set of state variables is by identifying the number of energy storage elements. With that, the n^{th} order of the system can also be known. For DC-DC boost converter, the circuit is a second order system with two state variables.

Boost converter is described by a set of state equations as in (5-6) corresponding to two different possible switching states. The switching states are defined as the duration of switch being turned on and turned off, namely the duty-cycle. The solution of the duty-cycle representation in state-space technique is obtained by summing up the terms for each switching mode (Mahmoud *et al.*, 2000). For example, let K for during switch to be turned on and (1-K) for the switch

turn off. The state variables are $[x_1(t)x_2(t)]^T = [i_L V_c]^T$. The state equation derivation for a boost converter $[\dot{X}_1 \dot{X}_2]^T = [i_L \dot{V}_c]^T$, is described by the following Eq.:

$$\dot{X}_1 = -\frac{1+K}{L}x_2 + \frac{1}{L}u \tag{7}$$

$$\dot{X}_2 = -\frac{1-K}{C}x_1 - \frac{1}{RC}x_2 \tag{8}$$

$$y = x_2 \tag{9}$$

The boost converter output current and the output power are expressed by:

$$I_o = \frac{V_o}{R} \tag{10}$$

$$P_o = V_o I_o \tag{11}$$

The state-space equations have been implemented in MATLAB/Simulink where the simulation block is illustrated in Fig. 5.

State-space averaging model for single-phase square-wave inverter:

The schematic of a typical single-phase full-bridge inverter is shown in Fig. 6. In full-bridge inverter, the switches cannot be turned on simultaneously but two pairs of switches (S_1 and S_2 ; S_3 and S_4) are turned on alternatively. In square-wave switching technique, the inverter circuit produces the square wave output voltage. It has simple control logic and the power switches only operate at much lower frequencies compared to switching frequency in other counterparts. The switching states are defined as the duration of switch being turned on and off to yield 50% of duty-cycle.

This study focuses on the comparison of the performance yield between the state-space model and circuitry model under that similar simulation condition. For the purpose of simulation, it was assumed that there is no deadbeat time during the switching states in the power inverter. When the switch of the upper left leg (S_1) and the switch of the lower right leg (S_2) is operated, the inverter circuit including the LC filter yield two state variables. The operation of the state-space model is described by Eq. 5 and 6. The switching states are defined as the duration of switch S_1 and S_2 being turned on and turned off. The solution of the switching representation in state-space technique is obtained by summing up the terms for each switching mode which has been discussed in the previous part.

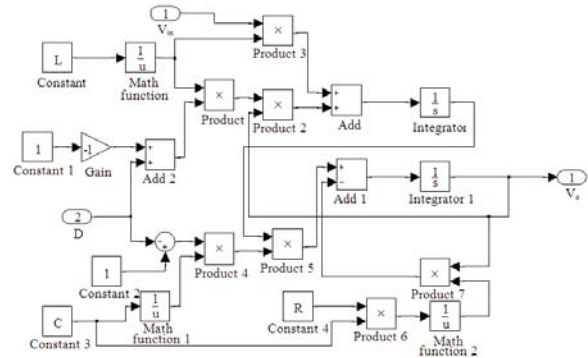


Fig. 5: Implementation of boost converter in MATLAB/Simulink

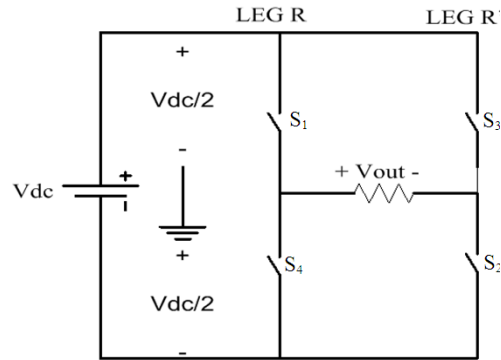


Fig. 6: The schematic diagram of a single-phase full-bridge inverter

Let D representing the duty-cycle during switch being turned on and (1-D) for the duration when the switch is turned off. Then, the state variables are $[x_1(t)x_2(t)]^T = [i_L V_c]^T$. The state equation derivation, $[\dot{X}_1 \dot{X}_2]^T = [i_L \dot{V}_c]^T$, for a single-phase square-wave inverter is described by Eq. 12-14:

$$\dot{X}_1 = -\frac{D}{L}x_2 + \frac{D}{L}u \tag{12}$$

$$\dot{X}_2 = -\frac{D}{C}x_1 + \frac{1}{RC}x_2 \tag{13}$$

$$y = x_2 \tag{14}$$

However, in the state-space model, the inverter model only yields the amplitude of the output voltage. In order to produce the sinusoidal waveform, the model needed to be multiplied with a sinusoidal equation, as expressed by the following:

$$V = V_m \sin(2\pi f)t \tag{15}$$

Where:

V_m = The peak voltage

t and f = The time and the output frequency

Similarly, the inverter model was developed using the MATLAB/Simulink. The simulation block for single-phase square-wave inverter is shown in Fig. 7.

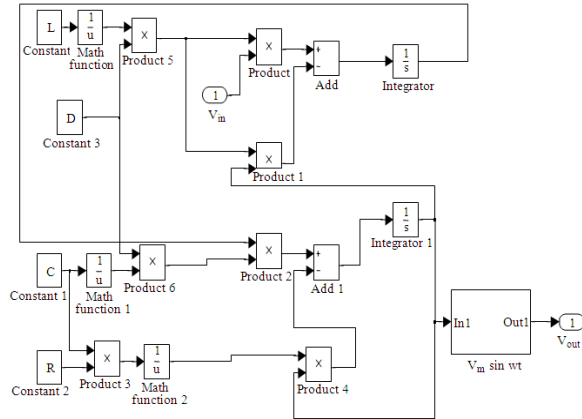


Fig. 7: Implementation of the single-phase square-wave inverter in MATLAB/Simulink

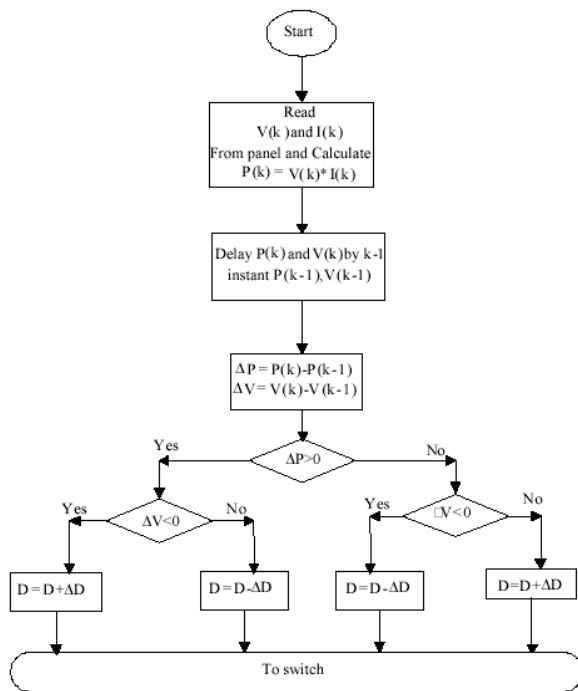


Fig. 8: The flowchart of P and O MPPT algorithm

Modeling of perturb and observe maximum power point algorithm:

The photovoltaic module yields the current-voltage characteristic with a unique point which is known as the Maximum Power Point (MPP) (Femia *et al.*, 2005). There are several MPP tracking methods in the literature, such as fuzzy logic control, neural network control, pilot cells and digital signal processor based implementation. Nevertheless, Perturb and Observe (P and O) and Incremental Conductance (INC) algorithms are most widely used, especially for low-cost implementations (Femia *et al.*, 2005; Mahmoud *et al.*, 2000; Marouani and Bacha, 2009).

As shown in the Fig. 2 and 3 in the previous part, the MPP changes as a consequence of the variation of the irradiance level and temperature. Therefore, it is necessary to ensure that the PV system always operates at the MPP in order to maximize the power harvesting the prevailing environmental conditions.

In P and O MPP algorithm, a small perturbation is introduced in every iteration to alter the duty cycle in order to force the operating point to move near the MPP. This algorithm compares the power measured in the previous cycle with the power of the current cycle to determine the next perturbation direction (Armstrong and Hurley, 2004). If the power increases due to the perturbation then the perturbation will remain in the same direction. If the operating point exceeds the peak power and deviate to the right side of the P-V characteristic curve, the power at the next instant will decrease, thus, the direction of the perturbation reverses. When the steady-state is reached, the operating point oscillates around the peak power (Armstrong and Hurley, 2004) as the MPP will perturb continuously. In order to keep the power variation small, the perturbation size is kept very small yet this will cause the system to respond slowly during transients. The operation of P and O MPP algorithm is illustrated in the Fig. 8 while Fig. 9 shows the designed MPPT in MATLAB/Simulink.

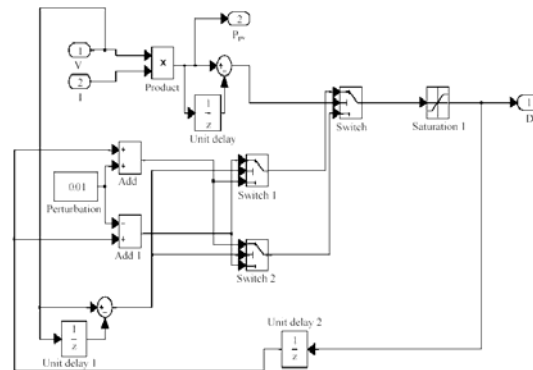


Fig. 9: P and O MPP simulink block

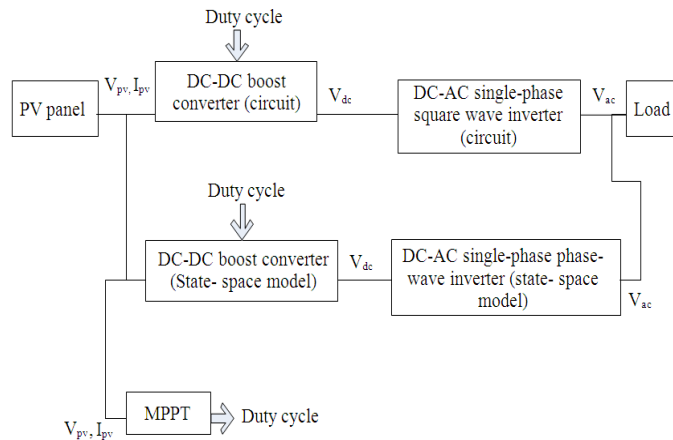


Fig. 10: A block diagram of the proposed PV system

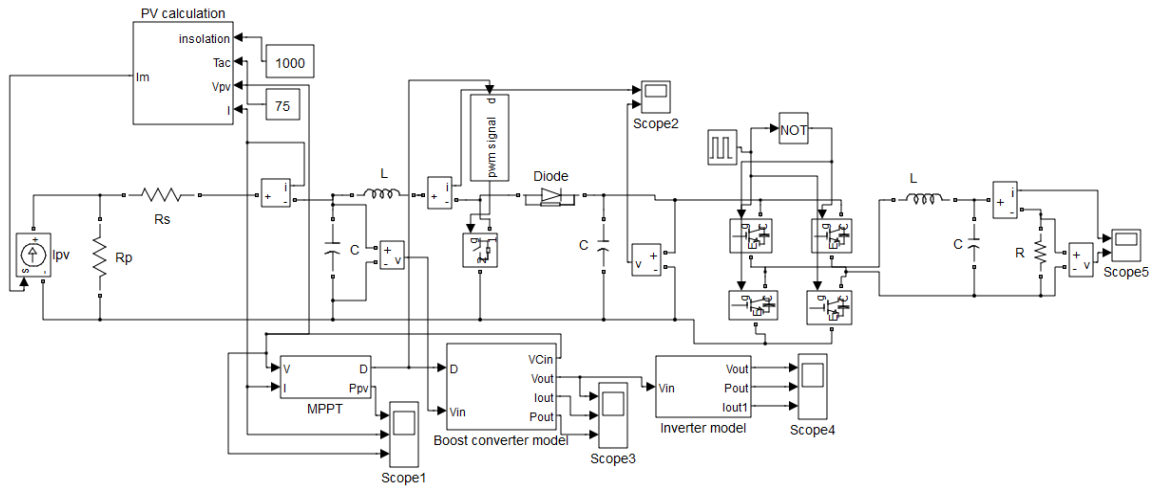


Fig. 11: The circuitry photovoltaic system developed in MATLAB/Simulink

Simulation setup: In order to validate the state-space model, a circuitry simulation of the proposed PV system is performed. This circuit is connected in parallel with the state-space model as shown in Fig. 10. Both the proposed PV state-space and circuitry models were developed in MATLAB/Simulink as shown in Fig. 11.

The DC-DC boost converter is designed to generate small output ripple less than 1%. The PV system was simulated under a variation of irradiance and temperature levels. The function of the MPPT block is to ensure that the system delivers the maximum power to the load by varying the duty ratio of the boost converter. The boost converter was designed to operate at the switching frequency of 20 kHz, the inductor of 20 mH, the output capacitor of 2 mF. The single-phase inverter was operated at switching frequency of 50 Hz, the inductor of 37 mH,

the capacitor of 450 μ F and the load is a pure resistive load of 10 Ω .

MATERIALS AND METHODS

Several simulations have been carried out using MATLAB/Simulink to test the effectiveness of proposed state-space PV system. The simulations were made to illustrate the response of the PV system for different temperature and solar irradiance levels for a duration of 0.35 sec. For this purpose, the irradiance, G, was initially set to change from 1000-600 Wm^{-2} and temperature was set to be constant as 25°C at the simulation time of 0.2 sec.

In the simulation, the proposed PV system was also tested under a sudden change of temperature with a constant solar irradiance of $G = 1000 \text{ W m}^{-2}$ and the temperature changes from $T = 25$ to -75°C at 0.2 sec.

RESULTS

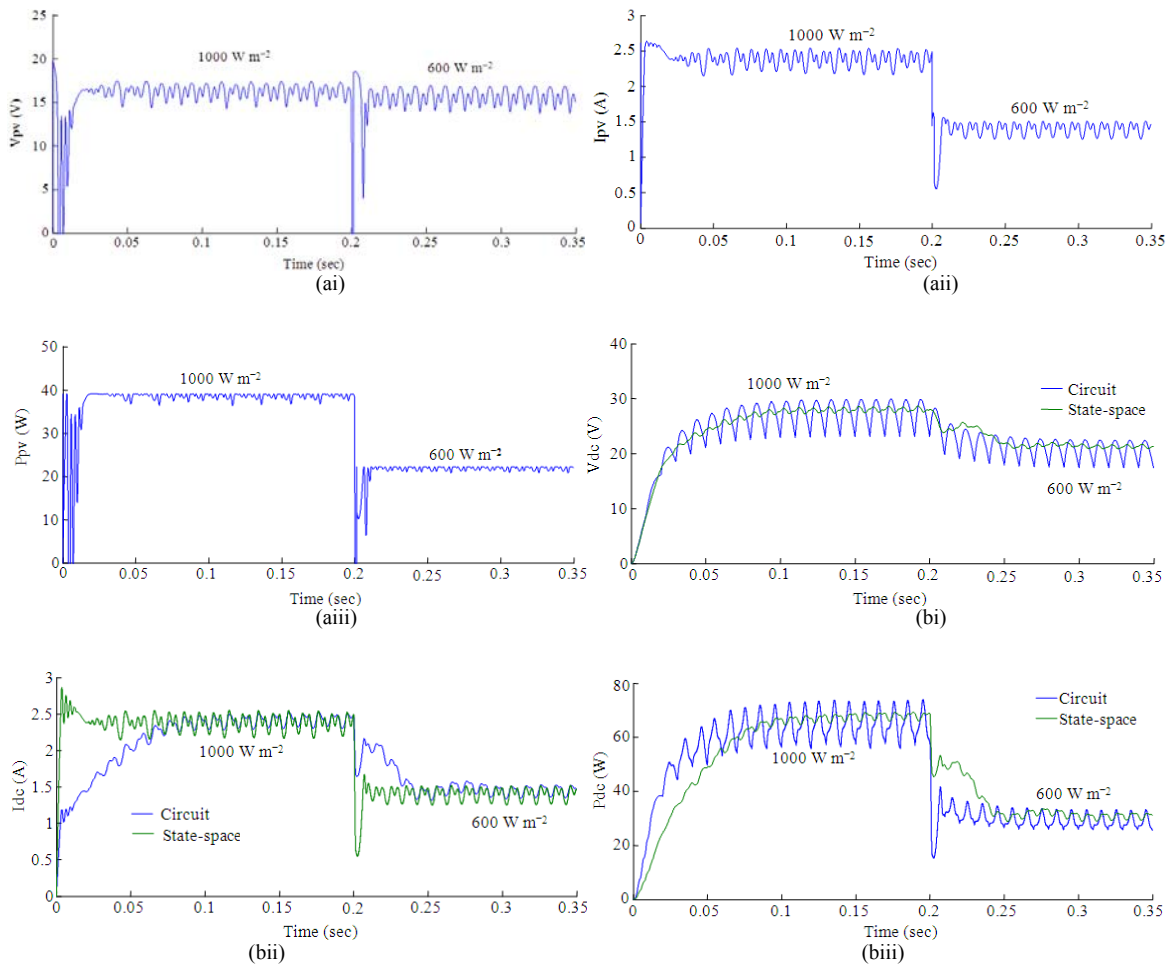
Figure 12a-c show the results of simulation at the output of PV, the DC-DC boost converter and DC-AC inverter side respectively, while Fig. 13a-c show the simulation results at the output of the PV source, DC-DC boost converter and DC-AC inverter side respectively.

DISCUSSION

The simulation results show that the PV model generates an average 43 W (note that the MPPT model is not the main focus in this study, the designed MPPT block does not yield ripple-free output waveform), 18 V of voltage and 2.3 A of current under the nominal maximum point (irradiance $G = 1000 \text{ W m}^{-2}$ and temperature $T = 25^\circ\text{C}$). This output value may change as the irradiance and temperature level changes as shown in Fig. 12a and 13a. Due to the fixed step-size used in the MPPT, the maximum power point tracking

controller brings the photovoltaic model continuously oscillates around the maximum power point. The oscillation occurs during the transient as shown in Fig. 12ai, aiii and 13ai, aiii are attributed to the switching action of boost converter and the fixed step-size of the P and O MPPT algorithm.

The results show that the state-space inverter model yields the similar waveform with the one produced by the circuitry simulation. The amplitude of the output waveform decreases when the irradiance and temperature of PV array decreased due to the voltage drop of the DC voltage of the boost converter. It can be noticed that there is a shift- delay appears at the inverter output waveform as shown in Fig. 12c and 13c. This is because, in state-space model, the inverter sinusoidal output waveform is produced by mathematical solution (Eq. 15) which is limited to the voltage amplitude; while in the circuitry model, the sinusoidal output waveform is produced by the LC filter circuit which the output is limited to the filter size.



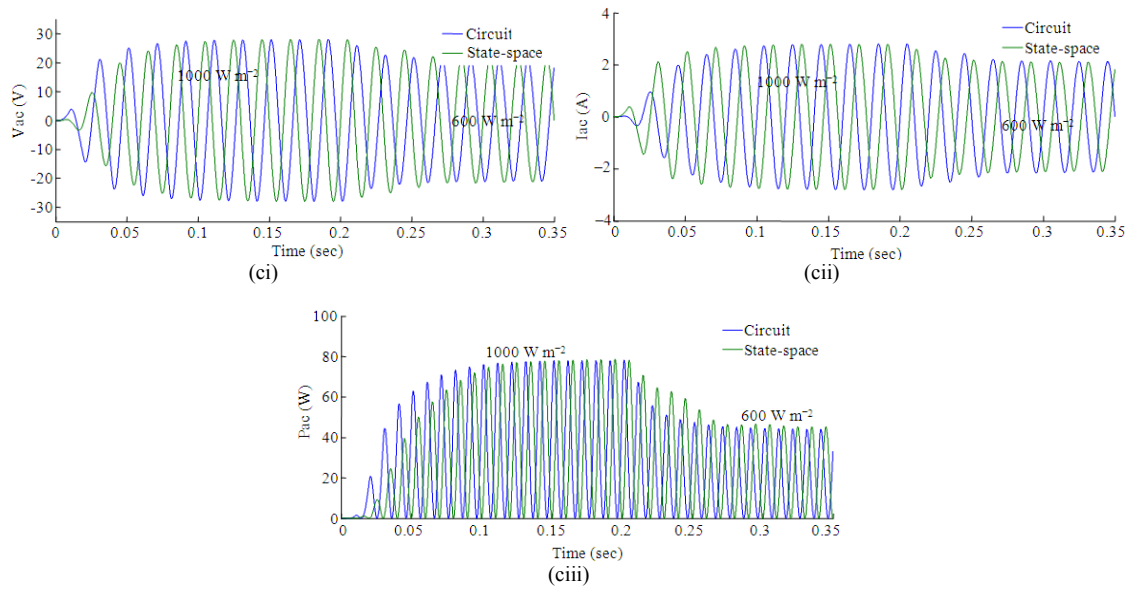
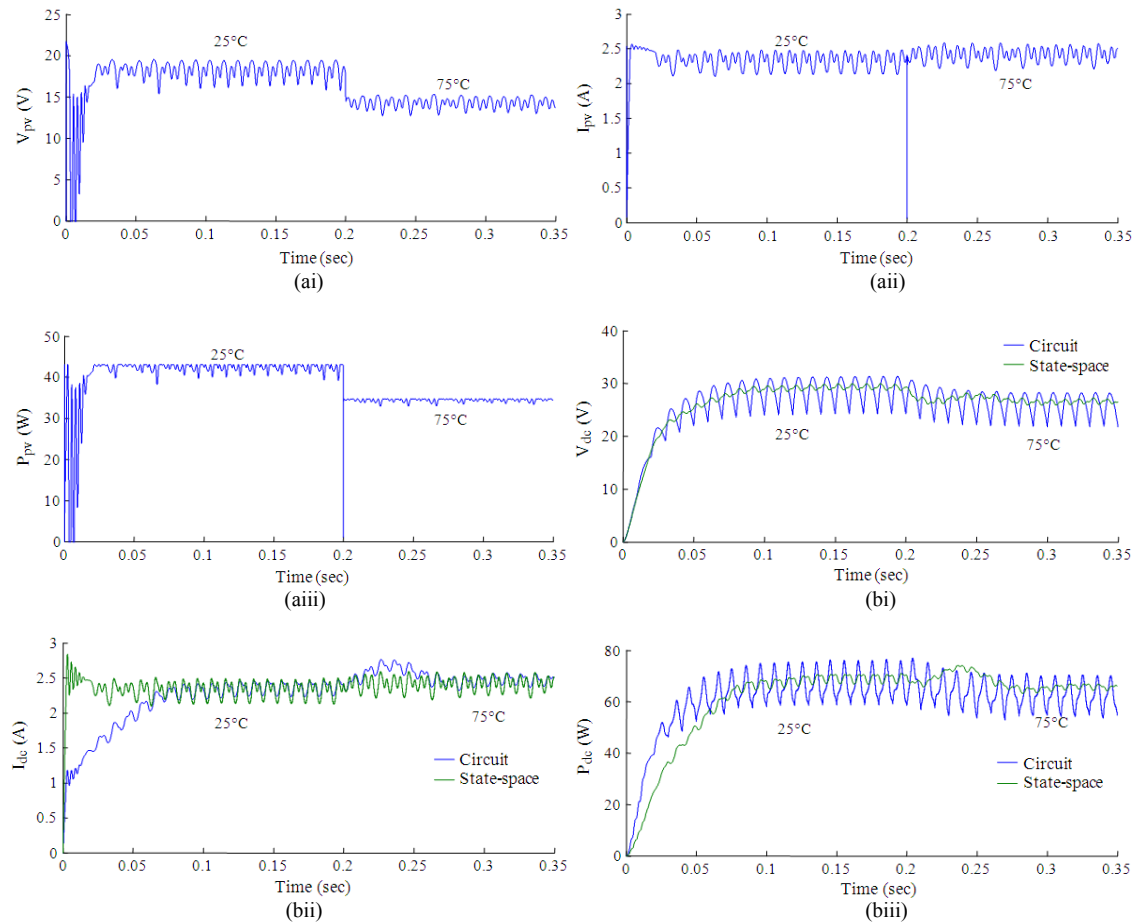


Fig.12: The simulation results with a step change of irradiance, $G = 1000\text{-}600 \text{ W m}^{-2}$ at the constant temperature, $T = 25^\circ\text{C}$: (a) PV side, (b) boost converter side, (c) inverter side



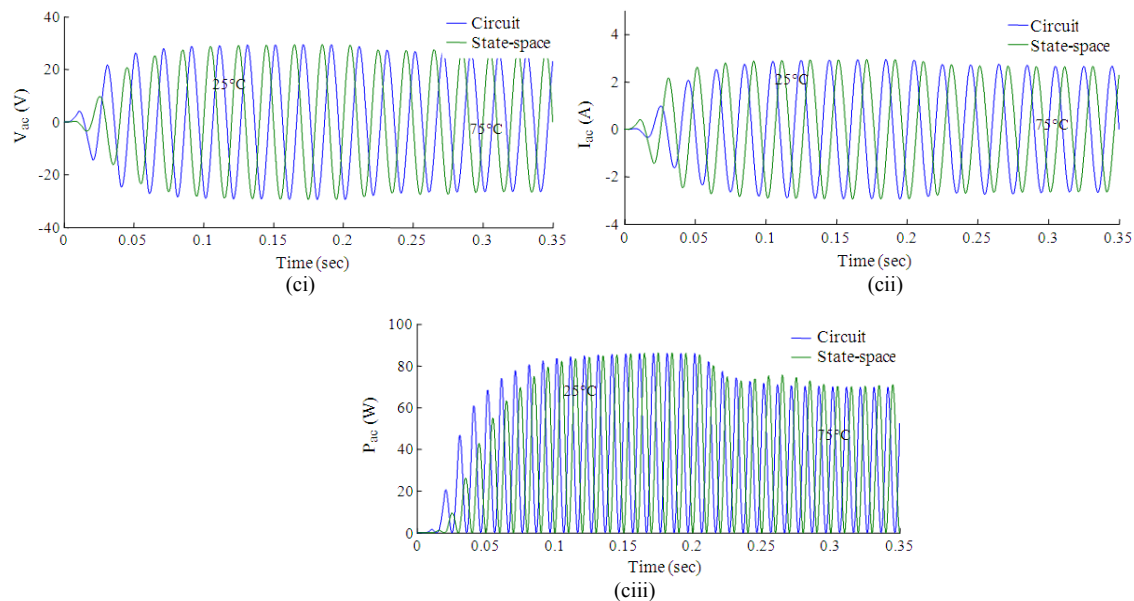


Fig. 13: The simulate ion results with a step-change of temperature, $T = 25$ to -75°C at the constant irradiance, $G = 1000 \text{ W m}^{-2}$: (a) PV side, (b) boost converter side, (c) inverter side

CONCLUSION

This study has presented the modeling of a stand-alone PV system using state-space averaging method. The details of the modeling technique and circuitry simulation were described and comparisons were made on both techniques. The objective of this method is to fit the mathematical equations to the system and validate with circuitry simulation for the purpose of comparison. Analysis of the results shows that the model yields the similar performance as produced by the circuitry simulation.

The state-space averaging technique is possible to implement in a modeling and control of photovoltaic system because the model yields the similar performance as the results from circuitry method which may help to reduce the overall simulation convergence time as state-space averaging method does not include the effect of switching that take longer simulation time to converge.

REFERENCES

Armstrong, S. and W.G. Hurley, 2004. Self-regulating maximum power point tracking for solar energy systems. Proceeding of the 39th International Universities Power Engineering Conference, Sept. 6-8, University of the West of England (UWE), Bristol, UK., pp: 1339-1350. <http://cat.inist.fr/?aModele=afficheN&cpsid=17707259>

Bae, H.S., J.H. Park, B.H. Cho and G.J. Yu, 2005. New control strategy for 2-stage utility-connected photovoltaic power conditioning system with a low cost digital processor. Proceedings of the IEEE 36th Power Electronics Specialists Conference, June 16-16, IEEE Xplore Press, pp: 2925-2929. <http://pearlx.snu.ac.kr/Publication/HSBae.pdf>

Chen, C.T., 1999. Linear System Theory. 3rd Edn., ISBN: 0-19-511777-8, pp: 86-98.

Femia, N., G. Petrone, G. Spagnuolo and M. Vitelli, 2005. Optimization of perturb and observe maximum power point tracking method. IEEE Trans. Power Elect., 20: 963-973. DOI: 10.1109/TPEL.2005.850975

Ito, R., Y. Matsuzaki, T. Tani and T. Yachi, 2003. Evaluation of performance of MPPT equipment in photovoltaic system. Proceeding of the 25th International Telecommunications Energy Conference, Oct. 19-23, IEEE Computer Society, USA., pp: 256-260. DOI: 10.1109/INTLEC.2003.1252122

Mahmoud, A.M.A., H.M. Mashaly, S.A. Kandil, H. El Khashab and M.N.F. Nashed, 2000. Fuzzy logic implementation for photovoltaic maximum power tracking. Proceeding of the 26th Annual Conference of the IEEE International Workshop on Robot and Human Interactive Communication, Oct. 22-28, IEEE Computer Society, pp: 735-740. DOI: 10.1109/IECON.2000.973240

- Marouani, R. and F. Bacha, 2009. A maximum-power-point tracking algorithm applied to a photovoltaic water-pumping system. Proceeding of the 8th International Symposium on Advanced Electromechanical Motion Systems and Electric Drives Joint Symposium, Sept. 2009, IEEE Computer Society, pp: 1-6. DOI: 10.1109/ELECTROMOTION.2009.5259078
- Moussa, W.M. and J.E. Morris, 1990. Comparison between state-space averaging and PWM switch for switch mode power supply analysis. Proceedings of the 1990 IEEE Southern Tier Technical Conference, Apr. 25-25, IEEE Xplore Press, Binghamton, NY., pp: 15-21. DOI: 10.1109/STIER.1990.324626
- Rashid, M.H., 2004. Power Electronics Circuits, Devices and Application. 3th Edn., Pearson/Prentice Hall, ISBN-10: 0131228153, pp: 880.
- Ropp, M.E. and S. Gonzalez, 2009. Development of a MATLAB/simulink model of a single-phase grid-connected photovoltaic system. IEEE Trans. Energy Conver., 24: 195-202. DOI: 10.1109/TEC.2008.2003206
- Salhi, R.E.B.M., 2009. Maximum power point tracking controller for PV systems using a PI regulator with boost DC/DC converter. ICGST-ACSE J., 8: 21-27. <http://www.icgst.com/acse/Volume8/Issue3/P1110710002.pdf>
- Theocharis, A.D., A. Menti, J. Miliadis-Argitis and T. Zacharias, 2005. Modeling and simulation of a single-phase residential photovoltaic system. Proceeding of the IEEE Russia Power Tech, June 27-30, IEEE Computer Society, St. Petersburg, pp: 1-7. DOI: 10.1109/PTC.2005.4524407
- Villalva, M.G., J.R. Gazoli and E.R. Filho, 2009. Comprehensive Approach to Modeling and Simulation of Photovoltaic Array. IEEE Trans. Power Elect., 25: 1198-1208. DOI: 10.1109/TPEL.2009.2013862